Search for Excited and Exotic Electrons in the $e\gamma$ Decay Channel in $p\overline{p}$ Collisions at $\sqrt{s} = 1.96$ TeV

D. Acosta,[16] J. Adelman,[12] T. Affolder,[9] T. Akimoto,[54] M.G. Albrow,[15] D. Ambrose,[43] S. Amerio,[42] D. Amidei,[33] A. Anastassov,[50] K. Anikeev,[31] A. Annovi,[44] J. Antos,[1] M. Aoki,[54] G. Apollinari,[15] T. Arisawa,[56] J-F. Arguin,[32] A. Artikov,[13] W. Ashmanskas,[15] A. Attal,[7] F. Azfar,[41] P. Azzi-Bacchetta,[42] N. Bacchetta,[42] H. Bachacou,[28] W. Badgett,[15] A. Barbaro-Galtieri,[28] G.J. Barker,[25] V.E. Barnes,[46] B.A. Barnett,[24] S. Baroiant,[6] M. Barone,[17] G. Bauer,[31] F. Bedeschi,[44] S. Behari,[24] S. Belforte,[53] G. Bellettini,[44] J. Bellinger,[58] E. Ben-Haim,[15] D. Benjamin,[14] A. Beretvas,[15] A. Bhatti,[48] M. Binkley,[15] D. Bisello,[42] M. Bishai,[15] R.E. Blair,[2] C. Blocker,[5] K. Bloom,[33] B. Blumenfeld,[24] A. Bocci,[48] A. Bodek,[47] G. Bolla,[46] A. Bolshov,[31] P.S.L. Booth,[29] D. Bortoletto,[46] J. Boudreau,[45] S. Bourov,[15] C. Bromberg,[34] E. Brubaker,[12] J. Budagov,[13] H.S. Budd,[47] K. Burkett,[15] G. Busetto,[42] P. Bussey,[19] K.L. Byrum,[2] S. Cabrera,[14] M. Campanelli,[18] M. Campbell,[33] A. Canepa,[46] M. Casarsa,[53] D. Carlsmith,[58] S. Carron,[14] R. Carosi,[44] M. Cavalli-Sforza,[3] A. Castro,[4] P. Catastini,[44] D. Cauz,[53] A. Cerri,[28] C. Cerri,[44] L. Cerrito,[23] J. Chapman,[33] C. Chen,[43] Y.C. Chen,[1] M. Chertok,[6] G. Chiarelli,[44] G. Chlachidze,[13] F. Chlebana,[15] I. Cho,[27] K. Cho,[27] D. Chokheli,[13] M.L. Chu,[1] S. Chuang,[58] J.Y. Chung,[38] W-H. Chung,[58] Y.S. Chung,[47] C.I. Ciobanu,[23] M.A. Ciocci,[44] A.G. Clark,[18] D. Clark,[5] M. Coca,[47] A. Connolly,[28] M. Convery,[48] J. Conway,[6] B. Cooper,[30] M. Cordelli,[17] G. Cortiana,[42] J. Cranshaw,[52] J. Cuevas,[10] R. Culbertson,[15] C. Currat,[28] D. Cyr,[58] D. Dagenhart,[5] S. Da Ronco,[42] S. D'Auria,[19] P. de Barbaro,[47] S. De Cecco,[49] G. De Lentdecker,[47] S. Dell'Agnello,[17] M. Dell'Orso,[44] S. Demers,[47] L. Demortier,[48] M. Deninno,[4] D. De Pedis,[49] P.F. Derwent,[15] C. Dionisi,[49] J.R. Dittmann,[15] P. Doksus,[23] A. Dominguez,[28] S. Donati,[44] M. Donega,[18] J. Donini,[42] M. D'Onofrio,[18] T. Dorigo,[42] V. Drollinger,[36] K. Ebina,[56] N. Eddy,[23] R. Ely,[28] R. Erbacher,[6] M. Erdmann,[25] D. Errede,[23] S. Errede,[23] R. Eusebi,[47] H-C. Fang,[28] S. Farrington,[29] I. Fedorko,[44] R.G. Feild,[59] M. Feindt,[25] J.P. Fernandez,[46] C. Ferretti,[33] R.D. Field,[16] I. Fiori,[44] G. Flanagan,[34] B. Flaugher,[15] L.R. Flores-Castillo,[45] A. Foland,[20] S. Forrester,[6] G.W. Foster,[15] M. Franklin,[20] J.C. Freeman,[28] H. Frisch,[12] Y. Fujii,[26] I. Furic,[12] A. Gajjar,[29] A. Gallas,[37] J. Galyardt,[11] M. Gallinaro,[48] A.F. Garfinkel,[46] C. Gay,[59] H. Gerberich,[14] D.W. Gerdes,[33] E. Gerchtein,[11] S. Giagu,[49] P. Giannetti,[44] A. Gibson,[28] K. Gibson,[11] C. Ginsburg,[58] K. Giolo,[46] M. Giordani,[53] G. Giurgiu,[11] V. Glagolev,[13] D. Glenzinski,[15] M. Gold,[36] N. Goldschmidt,[33] D. Goldstein,[7] J. Goldstein,[41] G. Gomez,[10] G. Gomez-Ceballos,[31] M. Goncharov,[51] O. González,[46] I. Gorelov,[36] A.T. Goshaw,[14] Y. Gotra,[45] K. Goulianos,[48] A. Gresele,[4] M. Griffiths,[29] C. Grosso-Pilcher,[12] U. Grundler,[23] M. Guenther,[46] J. Guimaraes da Costa,[20] C. Haber,[28] K. Hahn,[43] S.R. Hahn,[15] E. Halkiadakis,[47] A. Hamilton,[32] B-Y. Han,[47] R. Handler,[58] F. Happacher,[17] K. Hara,[54] M. Hare,[55] R.F. Harr,[57] R.M. Harris,[15] F. Hartmann,[25] K. Hatakeyama,[48] J. Hauser,[7] C. Hays,[14] H. Hayward,[29] E. Heider,[55] B. Heinemann,[29] J. Heinrich,[43] M. Hennecke,[25] M. Herndon,[24] C. Hill,[9] D. Hirschbuehl,[25] A. Hocker,[47] K.D. Hoffman,[12] A. Holloway,[20] S. Hou,[1] M.A. Houlden,[29] B.T. Huffman,[41] Y. Huang,[14] R.E. Hughes,[38] J. Huston,[34] K. Ikado,[56] J. Incandela,[9] G. Introzzi,[44] M. Iori,[49] Y. Ishizawa,[54] C. Issever,[9] A. Ivanov,[47] Y. Iwata,[22] B. Iyutin,[31] E. James,[15] D. Jang,[50] J. Jarrell,[36] D. Jeans,[49] H. Jensen,[15] E.J. Jeon,[27] M. Jones,[46] K.K. Joo,[27] S. Jun,[11] T. Junk,[23] T. Kamon,[51] J. Kang,[33] M. Karagoz Unel,[37] P.E. Karchin,[57] S. Kartal,[15] Y. Kato,[40] Y. Kemp,[25] R. Kephart,[15] U. Kerzel,[25] V. Khotilovich,[51] B. Kilminster,[38] D.H. Kim,[27] H.S. Kim,[23] J.E. Kim,[27] M.J. Kim,[11] M.S. Kim,[27] S.B. Kim,[27] S.H. Kim,[54] T.H. Kim,[31] Y.K. Kim,[12] B.T. King,[29] M. Kirby,[14] L. Kirsch,[5] S. Klimenko,[16] B. Knuteson,[31] B.R. Ko,[14] H. Kobayashi,[54] P. Koehn,[38] D.J. Kong,[27] K. Kondo,[56] J. Konigsberg,[16] K. Kordas,[32] A. Korn,[31] A. Korytov,[16] K. Kotelnikov,[35] A.V. Kotwal,[14] A. Kovalev,[43] J. Kraus,[23] I. Kravchenko,[31] A. Kreymer,[15] J. Kroll,[43] M. Kruse,[14] V. Krutelyov,[51] S.E. Kuhlmann,[2] N. Kuznetsova,[15] A.T. Laasanen,[46] S. Lai,[32] S. Lami,[48] S. Lammel,[15] J. Lancaster,[14] M. Lancaster,[30] R. Lander,[6] K. Lannon,[38] A. Lath,[50] G. Latino,[36] R. Lauhakangas,[21] I. Lazzizzera,[42] Y. Le,[24] C. Lecci,[25] T. LeCompte,[2] J. Lee,[27] J. Lee,[47] S.W. Lee,[51] R. Lefevre,[3] N. Leonardo,[31] S. Leone,[44] J.D. Lewis,[15] K. Li,[59] C. Lin,[59] C.S. Lin,[15] M. Lindgren,[15] T.M. Liss,[23] D.O. Litvintsev,[15] T. Liu,[15] Y. Liu,[18] N.S. Lockyer,[43] A. Loginov,[35] M. Loreti,[42] P. Loverre,[49] R-S. Lu,[1] D. Lucchesi,[42] P. Lujan,[28] P. Lukens,[15] G. Lungu,[16] L. Lyons,[41] J. Lys,[28] R. Lysak,[1] D. MacQueen,[32] R. Madrak,[20] K. Maeshima,[15] P. Maksimovic,[24] L. Malferrari,[4] G. Manca,[29] R. Marginean,[38] M. Martin,[24] A. Martin,[59] V. Martin,[37] M. Martínez,[3] T. Maruyama,[54] H. Matsunaga,[54] M. Mattson,[57] P. Mazzanti,[4] K.S. McFarland,[47] D. McGivern,[30] P.M. McIntyre,[51] P. McNamara,[50] R. NcNulty,[29] S. Menzemer,[31] A. Menzione,[44] P. Merkel,[15] C. Mesropian,[48] A. Messina,[49] T. Miao,[15] N. Miladinovic,[5] L. Miller,[20] R. Miller,[34] J.S. Miller,[33] R. Miquel,[28] S. Miscetti,[17] G. Mitselmakher,[16] A. Miyamoto,[26] Y. Miyazaki,[40] N. Moggi,[4] B. Mohr,[7] R. Moore,[15] M. Morello,[44] A. Mukherjee,[15] M. Mulhearn,[31] T. Muller,[25] R. Mumford,[24] A. Munar,[43] P. Murat,[15] J. Nachtman,[15] S. Nahn,[59] I. Nakamura,[43] I. Nakano,[39] A. Napier,[55] R. Napora,[24] D. Naumov,[36] V. Necula,[16] F. Niell,[33] J. Nielsen,[28] C. Nelson,[15] T. Nelson,[15] C. Neu,[43] M.S. Neubauer,[8] C. Newman-Holmes,[15] A-S. Nicollerat,[18] T. Nigmanov,[45] L. Nodulman,[2] O. Norniella,[3] K. Oesterberg,[21] T. Ogawa,[56] S.H. Oh,[14] Y.D. Oh,[27] T. Ohsugi,[22] T. Okusawa,[40] R. Oldeman,[49] R. Orava,[21] W. Orejudos,[28] C. Pagliarone,[44] E. Palencia,[10] F. Palmonari,[44] R. Paoletti,[44] V. Papadimitriou,[15] S. Pashapour,[32]

J. Patrick,[15] G. Pauletta,[53] M. Paulini,[11] T. Pauly,[41] C. Paus,[31] D. Pellett,[6] A. Penzo,[53] T.J. Phillips,[14] G. Piacentino,[44] J. Piedra,[10] K.T. Pitts,[23] C. Plager,[7] A. Pompoš,[46] L. Pondrom,[58] G. Pope,[45] O. Poukhov,[13] F. Prakoshyn,[13] T. Pratt,[29] A. Pronko,[16] J. Proudfoot,[2] F. Ptohos,[17] G. Punzi,[44] J. Rademacker,[41] A. Rakitine,[31] S. Rappoccio,[20] F. Ratnikov,[50] H. Ray,[33] A. Reichold,[41] B. Reisert,[15] V. Rekovic,[36] P. Renton,[41] M. Rescigno,[49] F. Rimondi,[4] K. Rinnert,[25] L. Ristori,[44] W.J. Robertson,[14] A. Robson,[41] T. Rodrigo,[10] S. Rolli,[55] L. Rosenson,[31] R. Roser,[15] R. Rossin,[42] C. Rott,[46] J. Russ,[11] A. Ruiz,[10] D. Ryan,[55] H. Saarikko,[21] S. Sabik,[32] A. Safonov,[6] R. St. Denis,[19] W.K. Sakumoto,[47] G. Salamanna,[49] D. Saltzberg,[7] C. Sanchez,[3] A. Sansoni,[17] L. Santi,[53] S. Sarkar,[49] K. Sato,[54] P. Savard,[32] A. Savoy-Navarro,[15] P. Schlabach,[15] E.E. Schmidt,[15] M.P. Schmidt,[59] M. Schmitt,[37] L. Scodellaro,[42] A. Scribano,[44] F. Scuri,[44] A. Sedov,[46] S. Seidel,[36] Y. Seiya,[40] F. Semeria,[4] L. Sexton-Kennedy,[15] I. Sfiligoi,[17] M.D. Shapiro,[28] T. Shears,[29] P.F. Shepard,[45] M. Shimojima,[54] M. Shochet,[12] Y. Shon,[58] I. Shreyber,[35] A. Sidoti,[44] J. Siegrist,[28] M. Siket,[1] A. Sill,[52] P. Sinervo,[32] A. Sisakyan,[13] A. Skiba,[25] A.J. Slaughter,[15] K. Sliwa,[55] D. Smirnov,[36] J.R. Smith,[6] F.D. Snider,[15] R. Snihur,[32] S.V. Somalwar,[50] J. Spalding,[15] M. Spezziga,[52] L. Spiegel,[15] F. Spinella,[44] M. Spiropulu,[9] P. Squillacioti,[44] H. Stadie,[25] A. Stefanini,[44] B. Stelzer,[32] O. Stelzer-Chilton,[32] J. Strologas,[36] D. Stuart,[9] A. Sukhanov,[16] K. Sumorok,[31] H. Sun,[55] T. Suzuki,[54] A. Taffard,[23] R. Tafirout,[32] S.F. Takach,[57] H. Takano,[54] R. Takashima,[22] Y. Takeuchi,[54] K. Takikawa,[54] M. Tanaka,[2] R. Tanaka,[39] N. Tanimoto,[39] S. Tapprogge,[21] M. Tecchio,[33] P.K. Teng,[1] K. Terashi,[48] R.J. Tesarek,[15] S. Tether,[31] J. Thom,[15] A.S. Thompson,[19] E. Thomson,[43] P. Tipton,[47] V. Tiwari,[11] S. Tkaczyk,[15] D. Toback,[51] K. Tollefson,[34] T. Tomura,[54] D. Tonelli,[44] M. Tönnesmann,[34] S. Torre,[44] D. Torretta,[15] S. Tourneur,[15] W. Trischuk,[32] J. Tseng,[41] R. Tsuchiya,[56] S. Tsuno,[39] D. Tsybychev,[16] N. Turini,[44] M. Turner,[29] F. Ukegawa,[54] T. Unverhau,[19] S. Uozumi,[54] D. Usynin,[43] L. Vacavant,[28] A. Vaiciulis,[47] A. Varganov,[33] E. Vataga,[44] S. Vejcik III,[15] G. Velev,[15] V. Veszpremi,[46] G. Veramendi,[23] T. Vickey,[23] R. Vidal,[15] I. Vila,[10] R. Vilar,[10] I. Vollrath,[32] I. Volobouev,[28] M. von der Mey,[7] P. Wagner,[51] R.G. Wagner,[2] R.L. Wagner,[15] W. Wagner,[25] R. Wallny,[7] T. Walter,[25] T. Yamashita,[39] K. Yamamoto,[40] Z. Wan,[50] M.J. Wang,[1] S.M. Wang,[16] A. Warburton,[32] B. Ward,[19] S. Waschke,[19] D. Waters,[30] T. Watts,[50] M. Weber,[28] W.C. Wester III,[15] B. Whitehouse,[55] A.B. Wicklund,[2] E. Wicklund,[15] H.H. Williams,[43] P. Wilson,[15] B.L. Winer,[38] P. Wittich,[43] S. Wolbers,[15] M. Wolter,[55] M. Worcester,[7] S. Worm,[50] T. Wright,[33] X. Wu,[18] F. Würthwein,[8] A. Wyatt,[30] A. Yagil,[15] U.K. Yang,[12] W. Yao,[28] G.P. Yeh,[15] K. Yi,[24] J. Yoh,[15] P. Yoon,[47] K. Yorita,[56] T. Yoshida,[40] I. Yu,[27] S. Yu,[43] Z. Yu,[59] J.C. Yun,[15] L. Zanello,[49] A. Zanetti,[53] I. Zaw,[20] F. Zetti,[44] J. Zhou,[50] A. Zsenei,[18] and S. Zucchelli,[4]

(CDF Collaboration)

[1] *Institute of Physics, Academia Sinica, Taipei, Taiwan 11529, Republic of China*
[2] *Argonne National Laboratory, Argonne, Illinois 60439*
[3] *Institut de Fisica d'Altes Energies, Universitat Autonoma de Barcelona, E-08193, Bellaterra (Barcelona), Spain*
[4] *Istituto Nazionale di Fisica Nucleare, University of Bologna, I-40127 Bologna, Italy*
[5] *Brandeis University, Waltham, Massachusetts 02254*
[6] *University of California at Davis, Davis, California 95616*
[7] *University of California at Los Angeles, Los Angeles, California 90024*
[8] *University of California at San Diego, La Jolla, California 92093*
[9] *University of California at Santa Barbara, Santa Barbara, California 93106*
[10] *Instituto de Fisica de Cantabria, CSIC-University of Cantabria, 39005 Santander, Spain*
[11] *Carnegie Mellon University, Pittsburgh, PA 15213*
[12] *Enrico Fermi Institute, University of Chicago, Chicago, Illinois 60637*
[13] *Joint Institute for Nuclear Research, RU-141980 Dubna, Russia*
[14] *Duke University, Durham, North Carolina 27708*
[15] *Fermi National Accelerator Laboratory, Batavia, Illinois 60510*
[16] *University of Florida, Gainesville, Florida 32611*
[17] *Laboratori Nazionali di Frascati, Istituto Nazionale di Fisica Nucleare, I-00044 Frascati, Italy*
[18] *University of Geneva, CH-1211 Geneva 4, Switzerland*
[19] *Glasgow University, Glasgow G12 8QQ, United Kingdom*
[20] *Harvard University, Cambridge, Massachusetts 02138*
[21] *The Helsinki Group: Helsinki Institute of Physics; and Division of High Energy Physics, Department of Physical Sciences, University of Helsinki, FIN-00044, Helsinki, Finland*
[22] *Hiroshima University, Higashi-Hiroshima 724, Japan*
[23] *University of Illinois, Urbana, Illinois 61801*
[24] *The Johns Hopkins University, Baltimore, Maryland 21218*
[25] *Institut für Experimentelle Kernphysik, Universität Karlsruhe, 76128 Karlsruhe, Germany*

2

[26] *High Energy Accelerator Research Organization (KEK), Tsukuba, Ibaraki 305, Japan*

[27] *Center for High Energy Physics: Kyungpook National University, Taegu 702-701; Seoul National University, Seoul 151-742; and SungKyunKwan University, Suwon 440-746; Korea*

[28] *Ernest Orlando Lawrence Berkeley National Laboratory, Berkeley, California 94720*

[29] *University of Liverpool, Liverpool L69 7ZE, United Kingdom*

[30] *University College London, London WC1E 6BT, United Kingdom*

[31] *Massachusetts Institute of Technology, Cambridge, Massachusetts 02139*

[32] *Institute of Particle Physics: McGill University, Montréal, Canada H3A 2T8; and University of Toronto, Toronto, Canada M5S 1A7*

[33] *University of Michigan, Ann Arbor, Michigan 48109*

[34] *Michigan State University, East Lansing, Michigan 48824*

[35] *Institution for Theoretical and Experimental Physics, ITEP, Moscow 117259, Russia*

[36] *University of New Mexico, Albuquerque, New Mexico 87131*

[37] *Northwestern University, Evanston, Illinois 60208*

[38] *The Ohio State University, Columbus, Ohio 43210*

[39] *Okayama University, Okayama 700-8530, Japan*

[40] *Osaka City University, Osaka 588, Japan*

[41] *University of Oxford, Oxford OX1 3RH, United Kingdom*

[42] *University of Padova, Istituto Nazionale di Fisica Nucleare, Sezione di Padova-Trento, I-35131 Padova, Italy*

[43] *University of Pennsylvania, Philadelphia, Pennsylvania 19104*

[44] *Istituto Nazionale di Fisica Nucleare, University and Scuola Normale Superiore of Pisa, I-56100 Pisa, Italy*

[45] *University of Pittsburgh, Pittsburgh, Pennsylvania 15260*

[46] *Purdue University, West Lafayette, Indiana 47907*

[47] *University of Rochester, Rochester, New York 14627*

[48] *The Rockefeller University, New York, New York 10021*

[49] *Istituto Nazionale di Fisica Nucleare, Sezione di Roma 1, University di Roma "La Sapienza," I-00185 Roma, Italy*

[50] *Rutgers University, Piscataway, New Jersey 08855*

[51] *Texas A&M University, College Station, Texas 77843*

[52] *Texas Tech University, Lubbock, Texas 79409*

[53] *Istituto Nazionale di Fisica Nucleare, University of Trieste/ Udine, Italy*

[54] *University of Tsukuba, Tsukuba, Ibaraki 305, Japan*

[55] *Tufts University, Medford, Massachusetts 02155*

[56] *Waseda University, Tokyo 169, Japan*

[57] *Wayne State University, Detroit, Michigan 48201*

[58] *University of Wisconsin, Madison, Wisconsin 53706*

[59] *Yale University, New Haven, Connecticut 06520*

We present a search for excited and exotic electrons (e^*) decaying to an electron and a photon, both with high transverse momentum. We use 202 pb^{-1} of data collected in $p\bar{p}$ collisions at $\sqrt{s} = 1.96$ TeV with the CDF II detector. No signal above standard model expectation is seen for associated ee^* production. We discuss the e^* sensitivity in the parameter space of the excited electron mass M_{e^*} and the compositeness energy scale Λ. In the contact interaction model, we exclude 132 GeV/c^2 $< M_{e^*} <$ 879 GeV/c^2 for $\Lambda = M_{e^*}$ at 95% confidence level (C.L.). In the gauge-mediated model, we exclude 126 GeV/c^2 $< M_{e^*} <$ 430 GeV/c^2 at 95% C.L. for the phenomenological coupling $f/\Lambda \approx 10^{-2}$ GeV^{-1}.

The particle content of the standard model (SM) is given by three generations of quarks and leptons, each containing an $SU(2)$ doublet. This fermion multiplicity motivates a description in terms of underlying substructure, in which all quarks and leptons consist of fewer elementary particles bound by a new strong interaction [1]. In this compositeness model, quark-antiquark annihilations may result in the production of excited lepton states, such as the excited electron, e^*. The SM may be embedded in larger gauge groups such as $SO(10)$ or $E(6)$, motivated by grand unified theories or string theory. These embeddings also predict exotic fermions such as the e^*, produced via their gauge interactions [1].

We search for associated ee^* production followed by the radiative decay $e^* \to e\gamma$. This mode yields the distinctive $ee\gamma$ final state, which is fully reconstructable with high efficiency and good mass resolution, and has small backgrounds. The evidence for e^* production would be the observation of a resonance in the $e\gamma$ invariant mass distribution. The contact interaction (CI) Lagrangian [1] describing the reaction $q\bar{q} \to ee^*$ is

$$ L = \frac{4\pi}{\Lambda^2} \bar{q}_L \gamma^\mu q_L \bar{E}_L \gamma_\mu e_L + h.c. \quad , \qquad (1) $$

where E denotes the e^* field and Λ is the compositeness scale. The gauge-mediated (GM) model Lagrangian describing the e^* coupling to SM gauge fields is [1]

$$ L = \frac{1}{2\Lambda} \bar{E}_R \sigma^{\mu\nu} \left[fg\frac{\vec{\tau}}{2} \cdot \vec{W}_{\mu\nu} + f'g'\frac{Y}{2}B_{\mu\nu} \right] e_L + h.c., \quad (2) $$

leading to the reaction $q\bar{q} \to Z/\gamma \to ee^*$. $\vec{W}_{\mu\nu}$ and $B_{\mu\nu}$ are the $SU(2)_L$ and $U(1)_Y$ field-strength tensors, g and g' are the corresponding electroweak couplings, and f and f' are phenomenological parameters where we set $f = f'$.

Direct searches for e^* production have been performed at HERA by the ZEUS [2] and H1 [3] experiments and by the LEP2 [4,5] experiments. Mass limits have been set using the GM model only. The most stringent LEP limits are set by the OPAL experiment, which has excluded $M_{e^*} < 207$ GeV/c^2 for $f/\Lambda > 10^{-4}$ GeV^{-1} and $M_{e^*} < 103.2$ GeV/c^2 for any value of f/Λ [5], all at 95% C.L.. The most stringent limits from HERA are set by the H1 experiment, excluding $M_{e^*} < 280$ GeV/c^2 at 95% C.L. for $f/\Lambda \sim 0.1$ GeV^{-1} [3]. In this Letter, we extend the sensitivity to higher values of M_{e^*}, for $f/\Lambda > 0.005$ GeV^{-1}. We present the first e^* search in the context of the CI model, and the first e^* search at a hadron collider.

We use 202 pb^{-1} of data collected by the CDF II detector [6] during 2001-2003, from $p\bar{p}$ collisions at $\sqrt{s} = 1.96$ TeV at the Fermilab Tevatron. The detector consists of a magnetic spectrometer with silicon and drift chamber trackers, surrounded by a time-of-flight system, pre-shower detectors, electromagnetic (EM) and hadronic (Had) calorimeters, and muon detectors. The main components used in this analysis are the central drift chamber (COT) [7], the central pre-shower detector [8] (for

detecting photon conversions), and the central [9] and forward [10] calorimeters. Wire and strip chambers [8] are embedded in the central EM calorimeter to measure transverse shower profiles for e/γ identification. The COT, central calorimeter and pre-shower detectors cover the region $|\eta| < 1.1$ and the forward calorimeters extend e/γ coverage to $|\eta| < 2.8$, where η is the pseudorapidity.

We trigger on central electron candidates based on high transverse-energy [11] EM clusters with associated high transverse-momentum [11] tracks, with an efficiency (governed by the track trigger requirement) of $(96.2 \pm 0.1)\%$. We also use a second electron trigger, with a higher E_T threshold, but with less restrictive identification requirements, which ensures $\approx 100\%$ efficiency for $E_T > 100$ GeV. In the offline analysis, we require two fiducial electron candidates (without charge criteria) and a photon candidate, each with $E_T > 25$ GeV. We require the isolation $I_{0.4} < 0.1$, where $I_{0.4}$ is the ratio of the total calorimeter E_T around the EM cluster within a radius of $R \equiv \sqrt{(\Delta\eta)^2 + (\Delta\phi)^2} = 0.4$ to the cluster E_T, and ϕ is the azimuthal angle. Longitudinal and lateral shower profiles are required to be consistent with the expectation for EM showers taken from test-beam data.

Central electrons are identified by requiring a matching COT track, while central photons are vetoed by a matching COT track with $p_T > (1 + 0.005 \times E_T/\text{GeV})$ GeV/c. Forward electrons and photons are not distinguished from each other by using tracking information (in order to maximize selection efficiency), but are collectively identified as forward EM objects. Events with any dielectron invariant mass in the range $81 < m_{ee} < 101$ GeV/c^2 are rejected to suppress $Z(\to ee)\gamma$ background.

We use a GEANT [12]-based detector simulation to obtain the offline identification efficiencies. The simulation is validated using an unbiased "probe" electron from $Z \to ee$ events that are triggered and identified using the other electron. We measure the central electron efficiency of $(94.0 \pm 0.3_{\text{stat}})\%$ from the data, compared to $(92.7 \pm 0.1_{\text{stat}})\%$ from the PYTHIA [14] simulation. The simulation of photons is validated by using the EM shower of the probe electron to emulate a photon. The measured "emulated photon" efficiency from data (simulation) is $75.5\% \pm 0.7_{\text{stat}}\%$ ($78.3\% \pm 0.2_{\text{stat}}\%$). The simulated efficiency of prompt photons is 76%, showing that the emulated photon is a good model for a real photon. The forward EM object efficiency is $89.0\% \pm 0.6_{\text{stat}}\%$ ($90.0\% \pm 0.6_{\text{stat}}\%$) in the data (simulation). The inefficiency (due to extraneous energy near the forward EM object) decreases with increasing E_T, falling below 1% for $E_T > 100$ GeV. Based on the data-simulation comparisons we assign a systematic uncertainty of 1% (3%) to the simulated central electron (photon) efficiency.

We calibrate the EM energy response by requiring the measured $Z(\to ee)$ boson mass to agree with the world average [13]. The simulated resolution is tuned using the observed width of the mass peak. We calculate the full

acceptance (including trigger, geometric, kinematic and identification efficiencies) using the detector simulation. We generate $ee^* \to ee\gamma$ events using PYTHIA [14] for the CI model, and the LANHEP [15] and COMPHEP [16] programs for the GM model. The acceptance increases from 15% at $M_{e^*} = 100$ GeV/c^2 to an asymptotic value of 33% at high mass, with the largest difference between the models of $\approx 5\%$ at $M_{e^*} = 200$ GeV/c^2. The dominant systematic uncertainties come from identification efficiency (2.6%), passive material (1.4%), and parton distribution functions (PDFs) (1.0%), for a total of 3.7%.
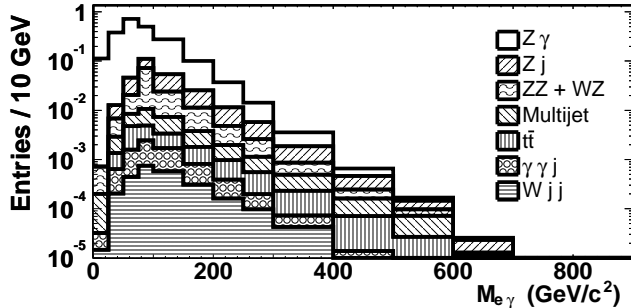

FIG. 1. The cumulative $e\gamma$ mass distribution for all backgrounds. Integrating over all masses, the total expected number of $e\gamma$ entries is 6.5 ± 0.1 (stat)$^{+0.9}_{-0.7}$ (syst).

Sources of background, in order of decreasing contribution, are production of (1) $Z\gamma \to ee\gamma$, (2) $Z(\to ee)+$ jet where the jet is mis-identified as a photon, (3) $WZ \to eee\nu$ and $ZZ \to eeee$ where an electron is mis-identified as a photon, (4) multi-jet events where jets are mis-identified as electrons and photons, (5) $t(\to e\nu b)\bar{t}(\to e\nu \bar{b})$ with energetic photon radiation off the b quarks, (6) $\gamma\gamma+$jet events, and (7) $W(\to e\nu) + 2$ jets where the jets are mis-identified as an electron and a photon.

We estimate the $Z\gamma$, WZ, ZZ, $t\bar{t}$ and $\gamma\gamma+$jet backgrounds using simulated events, with the ZGAMMA [17] generator for the $Z\gamma$ process and PYTHIA for the others. Their uncertainties are due to integrated luminosity (6%) [18], PDFs (5%), higher-order QCD corrections (5%) [19], identification efficiencies (1%-3%), passive material (4%) and energy scale and resolution (1%).

Backgrounds from $Z+$jet, $W + 2$ jet and multi-jet sources are estimated using data samples of such events, weighted by the measured "fake" rates for jets to be misidentified as electrons and photons. The photon fake rate is corrected for the prompt photon fraction in the jet sample, which is estimated using conversion signals observed in the calorimeter pre-shower detector. The central electron and photon fake rates are $\mathcal{O}(5 \times 10^{-4})$. The systematic uncertainty in the central photon fake rate ranges from $\sim 50\%$ at low E_T (due to variation with η) to a factor of ~ 2 at high E_T (due to statistical uncer-

TABLE I. Comparison of data and integrated background predictions above a given cut on the invariant mass of all $e\gamma$ combinations (left) and on the $ee\gamma$ invariant mass (right).

$e\gamma$ combinations			events		
$m_{e\gamma}$ cut	data	bkg.	$m_{ee\gamma}$ cut	data	bkg.
> 0 GeV/c^2	7	$6.5^{+0.9}_{-0.7}$	> 0 GeV/c^2	3	$3.0^{+0.4}_{-0.3}$
> 50 GeV/c^2	7	$5.3^{+0.8}_{-0.6}$	> 100 GeV/c^2	3	$2.3^{+0.4}_{-0.3}$
> 100 GeV/c^2	3	$2.3^{+0.4}_{-0.3}$	> 150 GeV/c^2	3	1.7 ± 0.3
> 150 GeV/c^2	3	$0.8^{+0.2}_{-0.1}$	> 200 GeV/c^2	2	0.9 ± 0.2
> 200 GeV/c^2	2	$0.31^{+0.10}_{-0.05}$	> 250 GeV/c^2	2	0.4 ± 0.1
> 250 GeV/c^2	1	$0.12^{+0.04}_{-0.02}$	> 300 GeV/c^2	2	$0.18^{+0.06}_{-0.04}$
> 300 GeV/c^2	0	$0.04^{+0.02}_{-0.01}$	> 350 GeV/c^2	0	$0.08^{+0.03}_{-0.02}$

TABLE II. Kinematics of the candidate events. e, γ, e' and j represent electron, photon, EM cluster and jet respectively. For forward EM objects, e and γ serve as distinguishing labels only. The fractional energy resolution for the central and forward calorimeters is given by sampling terms of $0.135\sqrt{\text{GeV}/E_T}$ and $0.16\sqrt{\text{GeV}/E}$ respectively, with constant terms of $\mathcal{O}(2\%)$. The η, ϕ and mass resolutions are ≈ 0.005, ≈ 0.003 and $\approx 3.5\%$ respectively. The jet in Event 3 is reconstructed with a cone radius $R = 0.4$, has its energy corrected for detector effects, and has energy and $\eta - \phi$ resolutions of $\approx 20\%$ and ≈ 0.01 respectively.

kinematic	Event 1	Event 2	Event 3
$E_T(e_1)$, charge(e_1)	37 GeV, +	44 GeV, −	164 GeV, +
$E_T(e_2)$, charge(e_2)	71 GeV, n.a.	42 GeV, −	94 GeV, −
$E_T(\gamma)$	48 GeV	46 GeV	72 GeV
$\eta(e_1), \phi(e_1)$	−1.01, 0.62	0.83, 3.64	−0.03, 1.73
$\eta(e_2), \phi(e_2)$	1.27, 4.05	−0.17, 1.96	0.46, 5.00
$\eta(\gamma), \phi(\gamma)$	−1.64, 2.02	1.47, 0.92	−0.29, 5.02
$m(e_1 e_2)$	176 GeV/c^2	78 GeV/c^2	256 GeV/c^2
$m(e_1\gamma)$	61 GeV/c^2	92 GeV/c^2	219 GeV/c^2
$m(e_2\gamma)$	257 GeV/c^2	92 GeV/c^2	64 GeV/c^2
$m(e_1 e_2\gamma)$	318 GeV/c^2	152 GeV/c^2	343 GeV/c^2
$E_T(e'/j)$		26 GeV	32 GeV
$\eta(e'/j), \phi(e'/j)$		1.53, 5.08	−0.50, 3.16
$m(e_2 e')$		92 GeV/c^2	

tainty on the prompt photon fraction). The fake rate for forward EM objects is an increasing function of η and E_T with value of $\mathcal{O}(10^{-2})$ and with systematic uncertainty of a factor of ~ 2 (due to variation with jet sample). All fake rates are applied as functions of E_T, and the forward EM object fake rate is also applied as a function of η. In the $Z-$veto region ($81 < m_{ee} < 101$ GeV/c^2) we observe 8 events and predict 5.8 ± 0.1 (stat) $^{+0.9}_{-0.5}$ (syst).

For the e^* resonance search, we compare the data with the expected background in a sliding window of $\pm 3\sigma$ width on the $e\gamma$ invariant mass distribution, where σ is the RMS of the e^* mass peak estimated from the simulation. All $e\gamma$ combinations are considered. The RMS is dominated by the detector resolution ($\approx 3.5\%$) over almost the entire e^* parameter space. Figure 1 shows the background predictions for $e\gamma$ combinations.

We find three candidate events, consistent with our

predicted background of 3.0 ± 0.1 (stat)$^{+0.4}_{-0.3}$ (syst). The systematic uncertainty receives equal contributions from the uncertainty on the SM backgrounds and the uncertainty on the mis-identification backgrounds due to the fake rates. Comparisons of data and backgrounds are shown in Table I. The kinematics of the candidates are presented in Table II. In Event 1 the forward "γ" has an associated track in the silicon detector and is consistent with being a negative electron. Event 2 has an additional EM cluster (e') that passes forward selection cuts but marginally fails the isolation cut ($I_{0.4} = 0.107$). Both forward objects have associated tracks in the silicon detector and are consistent with being positive electrons. The masses of the (e_1, γ) and (e_2, e') pairs are consistent with the event being a $Z(\to ee)Z(\to ee)$ candidate.

We set limits on e^* production using a Bayesian [13,20] approach, with a flat prior for the signal and Gaussian priors for the acceptance and background uncertainties. The 95% C.L. upper limits on the cross section $\times$ branching ratio (see Fig. 2) are converted into e^* mass limits by comparison with theory [19]. For both production models, the e^* decay is prescribed by the GM Lagrangian, which predicts BR($e^* \to e\gamma$) ≈ 0.3 for $M_{e^*} > 200$ GeV. We include mass-dependent uncertainties in the theoretical cross sections due to PDFs (5%-18%) and higher-order QCD corrections (7%-13%). Figure 3 shows the limits in the parameter space of f/Λ (M_{e^*}/Λ) versus M_{e^*} for the GM (CI) model. The region above the curve labeled "$\Gamma_{e^*} = 2M_{e^*}$" is unphysical for the GM model, because the total width Γ_{e^*} becomes larger than the mass.
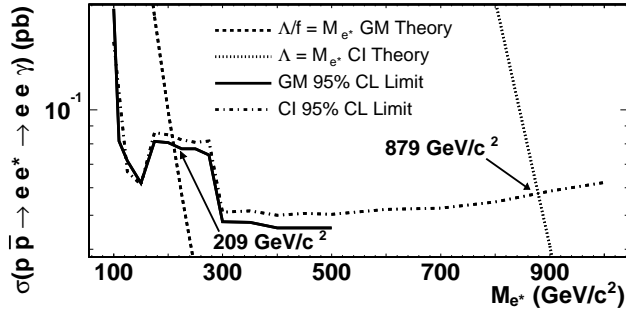
FIG. 2. The experimental cross section $\times$ branching ratio limits for the CI and GM models from this analysis, compared to the CI model prediction for $\Lambda = M_{e^*}$ and the GM model prediction for $\Lambda/f = M_{e^*}$. The mass limits are indicated.

In conclusion, we have presented the results of the first search for excited and exotic electrons at a hadron collider. We find three events, consistent with our predicted background. In the GM model, we exclude 126 GeV/c^2 $< M_{e^*} < 430$ GeV/c^2 for $f/\Lambda \approx 0.01$ GeV^{-1} at the 95% C.L., well beyond previous limits [2–5]. We have also presented the first e^* limits in the CI model as a func-

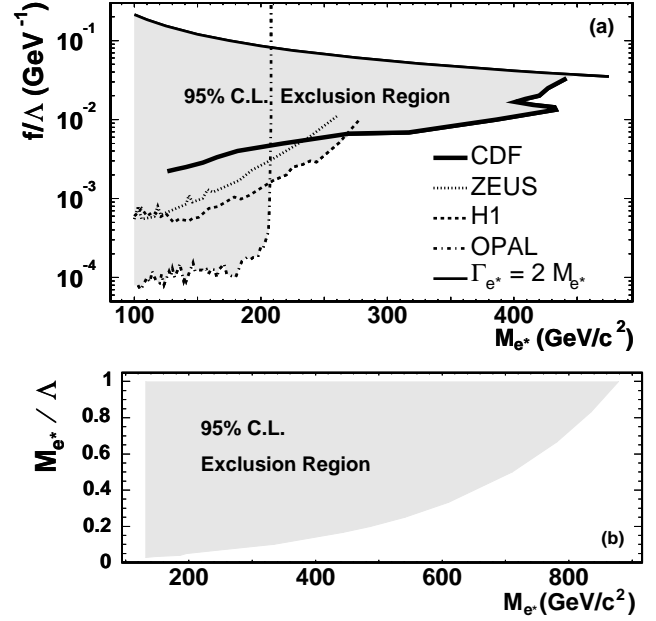tion of M_{e^*} and Λ, excluding 132 GeV/c^2 $< M_{e^*} < 879$ GeV/c^2 for $\Lambda = M_{e^*}$.

FIG. 3. The 2-D parameter space regions excluded by this analysis for (a) the GM model, along with the current world limits, and (b) the CI model.

[1] U. Baur, M. Spira and P. M. Zerwas, Phys. Rev. D **42**,

815 (1990), and references therein; E. Boos *et al.*, Phys. Rev. D **66**, 013011 (2002), and references therein.

[2] ZEUS Collaboration, S. Chekanov *et al.*, Phys. Lett. B **549**, 32 (2002).

[3] H1 Collaboration, C. Adloff *et al.*, Phys. Lett. B **548**, 35 (2002).

[4] ALEPH Collaboration, D. Buskulic *et al.*, Phys. Lett. B **385** , 445 (1996); DELPHI Collaboration, P. Abreu *et al.*, Eur. Phys. J. C **8** , 41 (1999); L3 Collaboration, P. Achard *et al.*, Phys. Lett. B **568**, 23 (2003).

[5] OPAL Collaboration, G. Abbiendi *et al.*, Phys. Lett. B **544**, 57 (2002).

[6] T. Affolder *et al.*, FERMILAB-Pub-96/390-E.

[7] T. Affolder *et al.*, Nucl. Instrum. Meth. Phys. Res. A **526**, 249 (2004).

[8] A. Byon-Wagner *et al.*, IEEE Trans. Nucl. Sci. **49**, 2567 (2002).

[9] CDF Collaboration, F. Abe *et al.*, Nucl. Instrum. Meth. Phys. Res. A **271**, 387 (1988).

[10] CDF Collaboration, M. G. Albrow *et al.*, Nucl. Instrum. Meth. Phys. Res. A **480**, 524 (2002); **431**, 104 (1999); P. de Barbaro *et al.*, IEEE Trans. Nucl. Sci. **42**, 510 (1995).

[11] "Transverse" energy (E_{T}) and momentum (p_{T}) imply the respective components perpendicular to the beam axis. Track p_{T} is obtained from its curvature, and $E_{\mathrm{T}} = E \sin \theta$, where E is the EM cluster energy.

[12] R. Brun and F. Carminati, CERN Program Library Long Writeup, W5013, 1993 (unpublished), version 3.15.

[13] K. Hagiwara *et al.* (Particle Data Group), Phys. Rev. D **66**, 010001 (2002).

[14] T. Sjöstrand, Comput. Phys. Commun. **82**, 74 (1994), version 6.127.

[15] A. V. Semenov, hep-ph/0208011 (2002); A. V. Semenov, Comput. Phys. Commun. **115**, 124 (1998).

[16] A. Pukhov *et al.*, hep-ph/9908288 (1999); E. E. Boos *et al.*, hep-ph/9503280 (1995).

[17] U. Baur and E. Berger, Phys. Rev. D **47**, 4889 (1993).

[18] S. Klimenko, J. Konigsberg, and T. M. Liss, Fermilab-FN-0741, December 2003 (unpublished); D. Acosta *et al.*, Nucl. Instrum. Meth. Phys. Res. A **494**, 57 (2002).

[19] U. Baur, T. Han and J. Ohnemus, Phys. Rev. D **57**, 2823 (1998); R. Hamberg, W. L. Van Neerven and T. Matsuura, Nucl. Phys. B **359**, 343 (1991), [Erratum-ibid. B **644**, 403 (2002)]; R. V. Harlander and W. B. Kilgore, Phys. Rev. Lett. **88**, 201801 (2002); A. Daleo, private communication. We use next-to-next-to-leading order cross sections evaluated with the MRST set of PDFs.

[20] I. Bertram *et al.*, Fermilab-TM-2104, April 2000 (unpublished).